INTERNATIONAL JOURNAL OF INTEGRATED ENGINEERING
ISSN: 2229-838X e-ISSN: 2600-7916

IJIE

Vol. 16 No. 1 (YEAR) 272-281
https://publisher.uthm.edu.my/ojs/index.php/ijie

A Reconfigurable Hardware Realization for Real-Time Simulation of Cardiac Excitation and Conduction

Farhanahani Mahmud[1,2]*, Nur Atiqah Adon[3], Norliza Othman[4], Ade Anggian Hakim[1], Marlia Morsin[1,2], Mohamad Hairol Jabbar[1]

[1] *Faculty of Electrical and Electronic Engineering, Universiti Tun Hussein Onn Malaysia (UTHM), 86400 Parit Raja, Batu Pahat, Johor, MALAYSIA*
[2] *Microelectronics and Nanotechnology Shamsuddin Research Centre (MiNT-SRC), Institute of Integrated Engineering (I2E), Universiti Tun Hussein Onn Malaysia (UTHM), 86400 Parit Raja, Batu Pahat, Johor, MALAYSIA*
[3] *Institut Kemahiran MARA (IKM), KM20 Jalan Bintulu-Sibu, 97000 Bintulu, Sarawak, MALAYSIA*
[4] *National Security Council State of Pahang, Bandar Indera Mahkota, 25200 Kuantan, Pahang, MALAYSIA*

*Corresponding Author: farhanah@uthm.edu.my
DOI: https://doi.org/10.30880/ijie.2024.16.01.022

Article Info

Received: 16 November 2023
Accepted: 3 March 2024
Available online: 22 May 2024

Keywords

FPGA, Virtex-6, cardiac excitation, reentrant, Luo-Rudy model, FitzHugh-Nagumo, HDL Coder

Abstract

Dynamic simulation of complex cardiac excitation and conduction requires high computational time. Thus, the hardware techniques that can run in real-time simulation were introduced. However, according to existing studies, the hardware simulation requires high power consumption and involves a large size of the physical parts. Due to the drawbacks, this research presents the adaptation of nonlinear Ordinary Differential Equation (ODE)-based cardiac excitable models of Luo-Rudy Phase I (LR-I) and FitzHugh-Nagumo (FHN) in a reconfigurable hardware of field-programmable gate array (FPGA). FPGA rapid prototyping using MATLAB Hardware Description Language (HDL) Coder was used to convert a fixed-point MATLAB Simulink blocks design of the cardiac models into a synthesizable VHSIC Hardware Description Language (VHDL) code and verified using the FPGA-In-the Loop (FIL) Co-simulator. The Xilinx FPGA Virtex-6 XC6VLX240T ML605 evaluation board was chosen as the FPGA platform. The cardiac excitation response characteristics using the LR-I model and the simulations of reentrant initiation and annihilation using the FHN model were verified in Virtex-6 FPGA. This means a new real-time simulation-based analysis technique of cardiac electrical excitation and conduction was successfully developed using the reconfigurable hardware.

1. Introduction

Cardiac arrest is caused by abnormalities in the cardiac electrical system such as arrhythmia [1,2] and its mechanism is difficult to understand. This situation leads to two techniques that have been used widely to study the underlying mechanism of the heart known as experimental and simulation techniques. The experimental technique is used to first build and then verify computational modeling which allows integration of past discoveries, quantitative computation of the models and the projection across relevant spatial and temporal scales [3]. However, the experimental technique has some drawbacks which are it needs a high quantity of variables for monitoring, high-resolution data in investigating larger proportions and is also costly [4].

Meanwhile, computer simulations are utilized for plausibility assessment, hypothesis generation, and prediction, which defining further the experimental research targets [3].

Advancement growth in the mathematical modeling of cardiac cells through mathematical descriptions of electrical events at the cellular level and its computer simulation has contributed to the use of simulations as a tool for studying cardiac dynamics. Furthermore, the computer simulation approach helps in reducing and replacing the use of animals in cardiac research [5]. Therefore, many mathematical models related to excitable media have been developed to represent different regions of the cardiac such as Hodgkin – Huxley [6,7], FitzHugh-Nagumo (FHN) model [8], Noble Purkinje model [9], Beeler and Reuter [10], and Luo-Rudy ventricular model [11-13]. Furthermore, Priebe Beukelmann (PB) [14] consists of 22 ODE variables, the Ten Tusscher-Noble-Panfilov [15] model consists of 17 ODE variables, and the Iyer-Mazhari-Winslow [16] model contains 67 ODE variables also have been developed to model the cell in more detail.

Thus far, the mathematical model has become more advanced from year to year as variable parameters increased to represent the model in more detail. Hence, this situation causes a new problem that needs a long time to compute the mathematical model. This scenario also gives problems with the computer simulation method, which requires a fast-speed computational computer, such as a supercomputer, to perform the simulations and raise the costs.

Alternatively, high-performance and low-power consumption hardware simulation provide valuable tools for electrophysiological applications such as in the medical and educational fields, considering their advantages of extremely fast and parallel mode execution, low power usage, reconfigurable, development ease, and low cost. One way to achieve a reduction in power consumption and size is by implementing the design using Very Large-Scale Integration (VLSI) technology [17]. For example, hardware tools that can be used for electrophysiological applications are Digital Signal Processing (DSPs), Field Programmable Gate Arrays (FPGAs), Graphical Processing Unit (GPU) and Application Specific Integrated Circuits (ASICs) [18]. Meanwhile, with the reliability requirements of biomedical instruments, FPGA embedded system development shows a trend of growth [19]. FPGA technology is now considered very useful by an increasing number of designers in various fields of application as it offers flexible, reconfigurable hardware, programmable circuit architecture, execution in parallel mode with a million gate counts, and low power consumption [20]. Moreover, it is also suitable for solving higher orders of Ordinary Differential Equations (ODEs) and high performance for real-time applications [21]. Recently, there are several existing studies on FPGA implementation for the analysis of excitable dynamics in neural systems [22-24]. However, there are still fewer studies on FPGA implementation for the analysis of excitable cardiac cell models. Therefore, this gives the motivation to implement the cardiac modeling on FPGA as it could realize a faster computation process compared to the software approach.

However, the designing process involves FPGA expertise in Very High-Speed Integrated Circuit (VHSIC) Hardware Description Language (VHDL) code. By manually writing the VHDL Code, it gives disadvantages as it is error-prone, time-consuming and high-level languages that are difficult to understand to a non-expertise on FPGA [25]. Nevertheless, in this research, MATLAB Hardware Description Language (HDL) Coder is used for faster FPGA prototyping. It is a software application from MathWorks that offers automatic HDL code generation from MATLAB Simulink design and code verification by using FPGA-in-the-Loop (FIL) approach.

Therefore, the present study intends to perform high-performance simulations of the cardiac cellular excitation and conduction based on the Luo-Rudy Phase I (LR-I) model and FitzHugh-Nagumo (FHN) model through MATLAB HDL Coder. The FPGA implementation of the cardiac mathematical model simulations contributes to accelerating the electrophysiology simulation in achieving real-time simulations of the cardiac mathematical models.

The rest of the paper is organized as follows. The methods are described in Section 2 where the design methodology and evaluation criteria for the FPGA-on-board simulation of the cardiac excitation and reentrant conduction are stated. The evaluation of results from the FPGA-on-board simulation which are according to the cardiac excitation response characteristics to periodic trains of stimuli and the reentrant mechanism, and the discussion based on the results are presented in Section 3. Finally, Section 4 summarizes the research work.

2. Methodology

There are two stages of work in the FPGA prototyping for real-time cardiac cell excitation and reentrant conduction simulations based on the cardiac models. The first stage involves FPGA design with fixed-point operations for the cardiac model simulation using the MATLAB HDL Coder. The LR-I model was firstly adapted and constructed by using MATLAB Simulink floating-point and converted into fixed-point. Then, the HDL Coder tool from MathWorks software was used for fixed-point and pipeline optimization before it was used to generate the VHDL code. Thirdly, the FPGA-in-the-Loop (FIL) co-simulation was performed to verify the generated code by HDL Coder. While the second stage involves the implementation of the FPGA design on the FPGA Virtex-6 XC6VLX240T ML605 evaluation board for the onboard simulations of the cardiac excitation using Xilinx Chipscope. For the execution on the FPGA board, the VHDL code was modified using the Xilinx ISE Design Suite

Int. Journal of Integrated Engineering Vol. 16 No. 1 (2024) p. 272-281

software by adding an IP core for Chipscope Pro to display the simulation output of cardiac cell excitation and reentrant conduction on the Chipscope Pro software. Then it was compiled, and the functionality of the code was analyzed using ISim software before it was programmed on the FPGA. Figure 1 shows the workflow of the FPGA implementation for the simulation of cardiac cell excitation.

The LR-I model [11] was chosen for this research for the simulation of a cardiac excitation while the FHN model was chosen for the cardiac reentrant conduction. The LR-I model is a well-known mathematical model used to simulate the electrical activity of cardiac cells which is a model of the mammalian cardiac ventricular action potential generation based mostly on the guinea pig ventricular cell. The LR-I model is described by a set of nonlinear ordinary differential equations (ODEs) that include eight dynamic state variables for describing six types of ion channel currents. Meanwhile, the FHN model is a universal cardiac cell excitable model that represents the depolarization and repolarization processes compactly and simply. This model is a good trade-off between complexity and computational efficiency and was chosen in this study to avoid computational difficulties often faced by researchers when using other models of cardiac tissue to represent the simulation of cardiac conduction. must be in MS Word only and should be formatted for direct printing, using the CRC MS Word provided. Figures and tables should be embedded and not supplied separately.

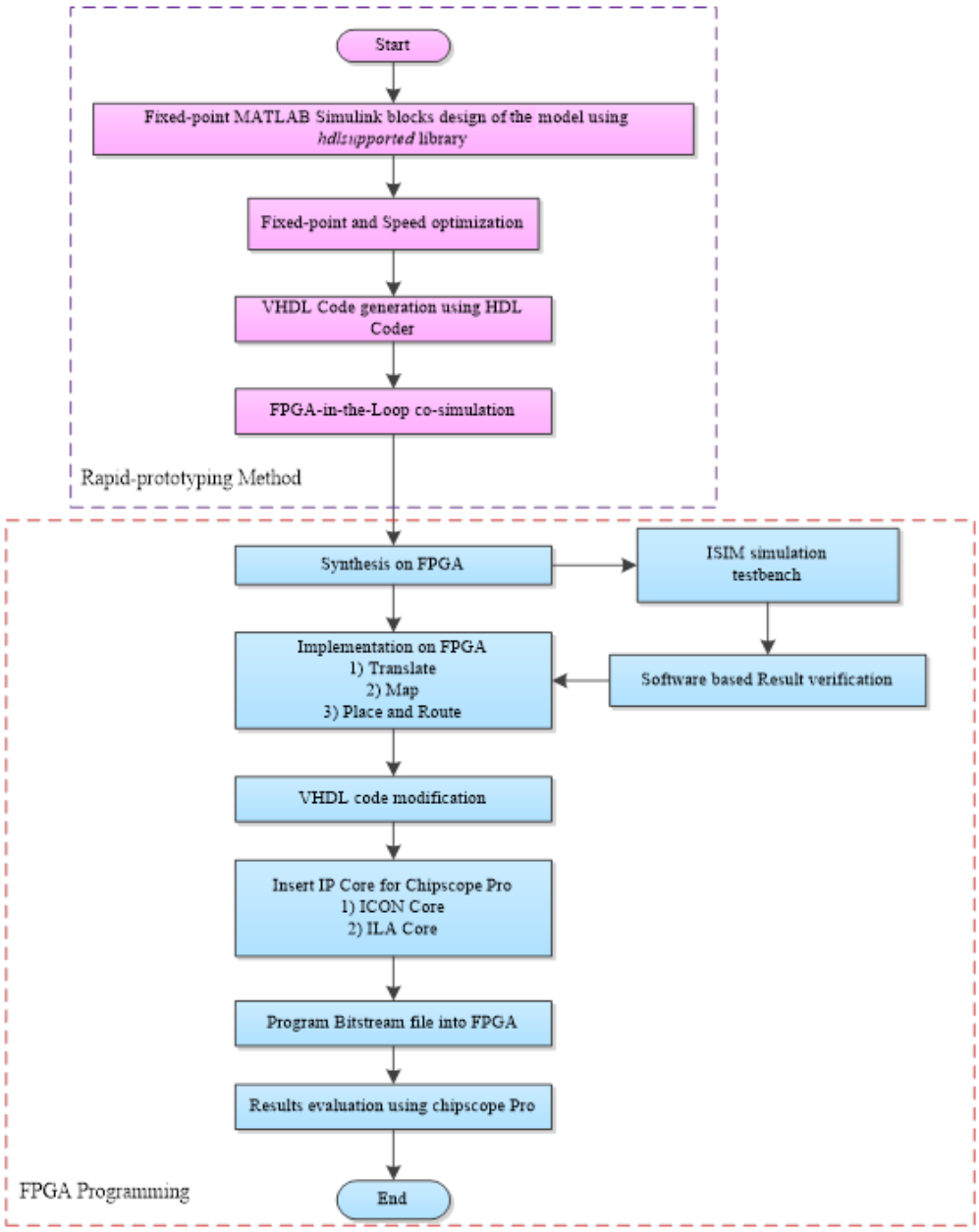

Fig. 1 *Workflow of the FPGA implementation for the simulation of the cardiac excitation and conduction*

2.1 FPGA Rapid Prototyping Design for the Simulation of the Cardiac Cell Excitation

For the realization of the reconfigurable hardware simulation for cardiac cell excitation using FPGA, MATLAB HDL Coder-based FPGA-rapid prototyping and Xilinx ISE-based rapid programming were conducted. The LR-I mathematical model was first adapted and constructed by using MATLAB Simulink floating-point and converted into the fixed-point operation. Fixed-point and pipelining optimization were also conducted before the FIL co-simulation of the cardiac excitation was performed to verify the cardiac excitation simulation in the fixed-point operation by the HDL Coder on the FPGA Virtex-6 XC6VLX240T ML605 evaluation board could give the same results as those from the MATLAB Simulink floating-point operation. Then, the generated code in VHDL from the HDL Coder was further improved in the Xilinx ISE Design Suite Software to suit the design requirement for the execution on the FPGA evaluation board which involved synthesis, translation and, place and route. The simulation output of the action potential for cellular excitation on the FPGA Virtex-6 was obtained from the Chipscope Pro. These design processes have been reported in detail in our previous work [26]. Based on the FPGA-on-board simulation, cardiac excitation response to periodic stimulation current trains with different intervals of time (t) and intensity of stimulation current (Isti) were compared to those of the computer simulation.

2.2 FPGA Rapid Prototyping Design for the Simulation of the Cardiac Reentrant Conduction

The workflow as in Fig. 1 was also implemented for the realization of the FPGA-on-board simulation for the cardiac reentrant conduction. One dimensional (1D) ring-shaped cable model with 80 cells of the FHN model designed using MATLAB Simulink blocks was able to be converted into synthesizable VHDL code by using an FPGA-based rapid-prototyping approach of MATLAB HDL Coder to simulate the reentrant conduction on the FPGA. Then, the VHDL design was functionally verified on an FPGA Xilinx Virtex-6 board using MATLAB HDL Verifier through FPGA-in-the-Loop (FIL) simulation approach before the simulation of reentrant conduction was conducted on Xilinx Chipscope Pro. The design process for the FPGA-on-board simulation of the cardiac reentrant conduction has been previously reported in [27]. Table 1 shows the FPGA Virtex-6 performance analysis conducted in the Xilinx ISE, for the cardiac excitation-conduction simulation in the 80 FHN cells 1D ring-shaped cable model in an optimum fixed-point data-type design with (word-length, WL, fraction-length, FL) of (24,22).

Table 1 *Hardware performance results of the 80 cells of the FHN model on the FPGA Virtex-6*

Parameters	80 cells
Number of slice registers	5536 (1.84%)
Number of slice LUTs	18, 632 (12.36%)
Number of DSP's	608 (79.17%)
Maximum frequency [MHz]	18.18
Power consumption [mW]	469

2.3 Evaluation Criteria

The performance evaluation of the FPGA-on-board simulations on the cardiac excitation and the 1D reentrant conduction in 1D ring-shaped cable model was done by comparing it with the performance of MATLAB based computer system. Several simulations on the cardiac excitation according to periodic trains of stimuli and the reentrant conduction which includes reentrant initiation and annihilation were conducted to compare the performance of our developed simulation method with the results from the computer simulations presented by the MATLAB programming. The simulation execution time performance between both methods is also compared. Besides, based on the simulation of the reentrant conduction, an analysis between a phase reset of the reentry and a phase of an applied single impulse was also conducted, and a Phase Resetting Curve (PRC) was also produced.

2.3.1 Phase Resetting Curve (PRC)

The result of detailed examinations on the responses of the reentrant to stimulations delivered in various phases can be analyzed using PRC as performed in the software-based computer simulation and FPGA-on-board simulation. The potential use of the PRC is to predict the effects of periodic stimuli on reentrant excitation wave circulating around in a loop. To this end, the phase of the reentrant wave is defined based on the time instant when the reentrant action potential is located at a given recording site. Through this study, the recording site is

Int. Journal of Integrated Engineering Vol. 16 No. 1 (2024) p. 272-281

located the same as the stimulation site, in compartment number i = 20. Firstly, the stimulation phase, which takes a value between 0 and 1, is interpreted as Equation 1.

$$\varphi = \frac{t_{stim}}{\overline{T}} \tag{1}$$

Where,
φ: Stimulation phase
t_{stim}: Time elapsed from the time instant when the last propagating reentrant action potential is detected at the recording site before the stimulation is applied.
$\overline{T}$: Period of the steady state reentry with no stimulations

Secondly, the amount of phase reset, $\Delta\varphi$ in response to stimulation with its phase, φ is defined as Equation 2.

$$\Delta\varphi = \frac{\Delta T}{\overline{T}} \tag{2}$$

Where,
$\Delta\varphi$: Phase reset
ΔT: The difference between the expected time instant of detecting the original reentrant action potential (when no stimulation is applied) and the time instant of detecting the reentrant action potential that is affected or newly generated by the stimulation. Positive and negative ΔT correspond to phase delay and advance, respectively.
$\overline{T}$: Period of the steady state reentry with no stimulations

3. Results and Discussion

In this section, the comparison between the simulation results of the cardiac excitation of the LR-I model according to periodic trains of stimuli and the reentrant conduction based on the 1D ring-shaped cable models consisting of 80 cells of the FHN model, obtained from the conventional MATLAB Simulink software-based computer simulation and the FPGA-on-board simulation using Chipscope system with a sample time of 0.001 ms are presented and discussed. This is to evaluate the performance of the developed FPGA system in terms of the simulation accuracy and the computational time performance. The study results on the phase resetting mechanism of the reentrant conduction are also presented. Moreover, the results obtained from the Chipscope Pro shown in Table 2 and Fig. 2 in the following subsections of 3.1 and 3.2.1, respectively are based on the number of samples. The number of samples can be represented by Equation 3. As an example, for 2000 ms of simulation time with a sample time of 0.001 ms, it will produce 2,000,000 numbers of samples.

$$\text{number of samples} = \frac{\text{simulation time}}{\text{sample time}} \tag{3}$$

3.1 Evaluation of the FPGA-on-board Simulation of the Cardiac Electrical Excitation

In this study, the FPGA-on-board simulations of action potential response to periodic stimulation current trains with different intervals of time (t) of 500 ms, 250 ms, 100 ms and 75 ms and intensity of stimulation current (Isti) of -80 μA and -50 μA were compared to those of the computer simulation. Here, the negative value of the Isti indicates the flow direction of the current from extracellular to intracellular. Table 2 shows the action potential generation according to the periodic stimulation current with the intensity of stimulation current of -80 μA and -50 μA, given with the intervals of time 500 ms, 250 ms, 100 ms and 75 ms.

Moreover, for the comparison of the results from the FPGA-on-board simulation and the MATLAB computer simulation, the results obtained from the developed FPGA-based simulation system through Chipscope Pro logic analyzer and from the MATLAB computer simulation system, respectively, are shown side by side, on the left side and the right side. The ratio at the right side of each of the graphs indicates the ratio of the number of applied stimulation currents to the complete action potential (AP) generated. For example, the ratio of 1:1 shows that each stimulation current enables the generation of a complete AP; meanwhile, for the ratio of 2:1, 4:1, and 5:1, in every two, four, and five current stimuli respectively applied, only one complete AP can be generated.

The irregular response patterns show the non-uniformity of the AP responses to particular repetitive impulse stimulations with a relatively small interval of time. This may imply to refractoriness of a cell, the condition in which the cell cannot fully induce the action potential wave before it has regained excitability and it could be noted clearly that the high intensity of the stimulation is more likely to produce irregular AP waves, while the low intensity of the stimulation could generate no AP waves. Moreover, a long interval of the stimulation period can produce a complete AP wave in every stimulation given, while a short periodic stimulation current will cause less complete generation of the AP waves and will cause a prolonged action potential duration (APD).

By comparing the response patterns between the two simulation techniques, it could be recognized that the FPGA-on-board simulation could simulate almost comparable action potential waveforms to those of computer simulation of the LR-I model. Furthermore, a small difference in the waveforms between the FPGA-on-board simulation and computer simulation results is because of the type of solver difference, in which the type of solver used in the FPGA-based system is the fixed-step solver and in the MATLAB simulation system is the variable-step solver.

Table 2 *Action potential generation based on of periodic trains of stimuli with the intensity of stimulation currents (I_{sti}) of -80 µA and -50 µA, with intervals of time (t) of 500 ms, 250 ms, 100 ms and 75 ms*

I_{sti} / t	-80 µA	-50 µA
500 ms	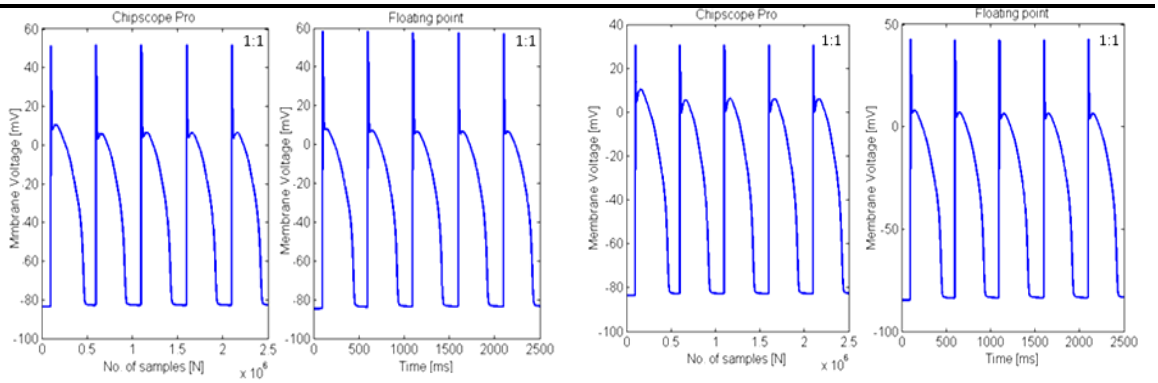	
250 ms	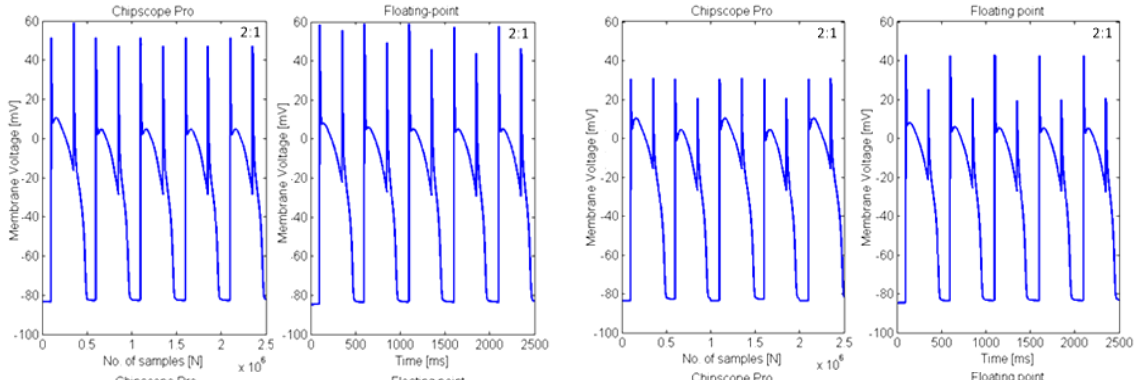	
100 ms	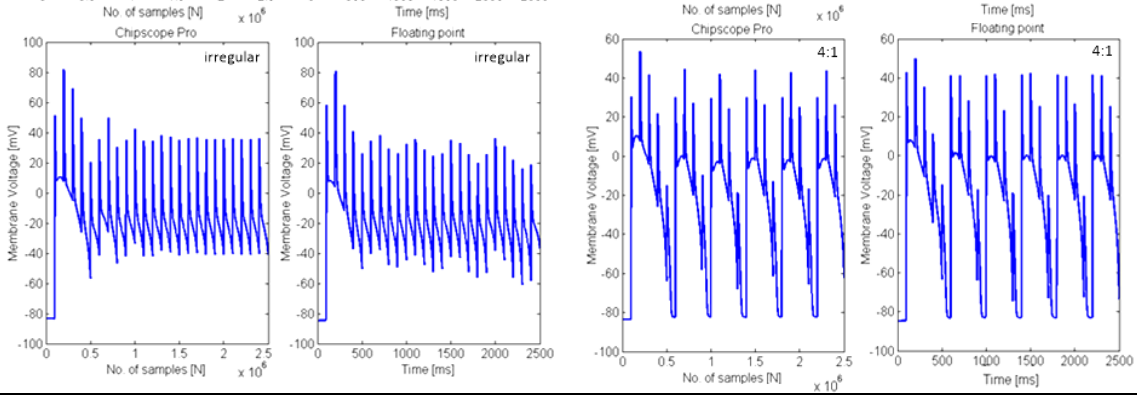	

Int. Journal of Integrated Engineering Vol. 16 No. 1 (2024) p. 272-281

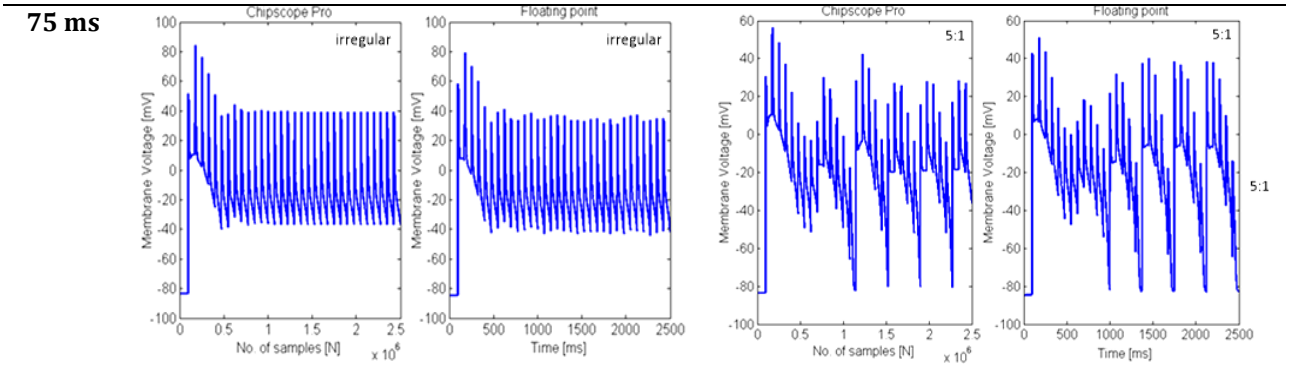

Furthermore, it is interesting to note that the simulation of the cardiac excitation based on the conventional software-based computer simulation technique using MATLAB was conducted with the 64-bit operating system and 16.0 GB of Installed Memory (RAM) on Intel® Xeon® CPU E5-2620 PC. The Ordinary Differential Equations (ODEs) from the Luo-Rudy Phase I (LR-I) model, which have been solved using MATLAB ode45 differential equation solver function based on a variable-step explicit Runge-Kutta method, can be run with a computational time of approximately 20 seconds for a floating-point model of simulation time set by 2500 ms. Meanwhile, through the Xilinx FPGA Virtex-6 evaluation board, the simulation of the cardiac excitation based on the 0.001 ms fixed time step discrete solver with the simulation time set by 2500 ms can run in a real-time (254 ns) with the on-board operating frequency of only 9.819MHz. Moreover, it is important to emphasize that the FPGA-based simulation could always operate in real-time, although there is an increase in the number of cell models and mathematical operations since FPGAs are truly parallel in nature.

3.2 Evaluation of the FPGA-on-board Simulation of the Reentrant Conduction

In this study, the FPGA-on-board simulations according to reentrant conduction also had been conducted. Started with the FPGA-on-board simulation on the initiation and annihilation of reentrant in 1D ring-shaped cable model and followed with the analysis of phase resetting curve (PRC) of the reentrant, the evaluation of the FPGA-on-board simulations was done by comparing the results from the FPGA-on-board simulation with those from the software-based computer simulation. The outcomes from the evaluations are explained in the following two subsections of 3.2.1 and 3.2.2.

3.2.1 Initiation and Annihilation of Reentrant in the Ring-shaped Cable Model

Figure 2 illustrates space-time diagrams representing the responses of the reentrant excitation to single stimulations in the ring-shaped cable model as a function of time and position obtained from the two simulation platforms. According to Fig. 2(a) and Fig. 2(b), two stimulations S1 were applied to the ring-shaped cable models at the number of cell compartments or i = 1, at time t = 100 ms and t = 350 ms (red arrows marked the area). Each stimulus evokes excitation at the stimulated site, which generates two conducting action potentials around both sides of the ring (clockwise directions and counterclockwise directions). As usual in excitable media, each conducting action potential possesses its wavefront and tail. The wavefront progressively excites the compartments ahead of the wavefront, and the wave tail is accompanied by refractoriness that decreases as being distant from the action potential. These action potentials collide with each other at the opposite side (in the ring state) of the stimulated, resulting in the annihilation of the reentry. Then, corresponding to an ectopic focus excitation in the real cardiac system, the S2 was applied at the cell compartment number i = 20 that slightly offset from the S1 site at an appropriate time interval after the second stimulation of S1.

Corresponding to Fig. 2(a), S2 was applied at t = 466 ms within a 116 ms time interval between S1 and S2 meantime in Fig. 2(b), S2 was applied at t = 460 ms with a time interval of 110 ms during after S1 stimulation. The reaction excitation wave attempts to propagate in both directions around the ring, but the excitability has regained on the other side because of insufficient recovery from the previous excitation wave. As a result, the wave conducted to the unidirectional block and blocks in the other direction. Since the excitation wave by the S1 has annihilated eventually, only the single wave of S2 remains, thereby initiating circus movement reentry.

Next, when a stimulus is delivered at an appropriate time interval referred to here as the annihilation interval, at which the stimulation site is located slightly away from the wave tail of the original reentry, the reentry can be annihilated. This was conducted by applying S3 also at the cell compartment number i = 20, at time t = 1540 ms and t = 1564 ms (red arrows marked the area shown in Fig. 2(a) and (b)), corresponding to the software-based computer simulation and FPGA-on-board simulation, respectively. This stimulus has been

generating a single action potential propagating only in one direction to collide with the originally propagating reentrant action potential wave leading to the annihilation of the reentry.

By comparing the response patterns in the two platforms of simulations, the result of the annihilation of the reentrant in the ring-shaped cable from the FPGA-on-board simulation is also comparable to that from the MATLAB software-based computer simulation. Moreover, the simulation of the reentrant mechanism based on the conventional MATLAB software-based computer simulation technique using MATLAB was conducted with 64-bit operating system and 8.0 GB of Installed Random Access Memory (RAM) on Intel® Core ™ i7-3770 processor Personal Computer (PC). The Ordinary Differential Equations (ODEs) from the FHN model, which were solved by MATLAB ode23 differential equation solver function based on a variable-step explicit Runge-Kutta method of the Dormand-Prince pair formula, can be run with an execution time of 4.85 sec for a simulation time set by 2000 ms. While, through the Xilinx Virtex-6 FPGA board the simulation of the reentrant mechanism based on the 0.001 ms fixed time step discrete solver can be run in real-time with the on-board maximum operating frequency of only 200 MHz.

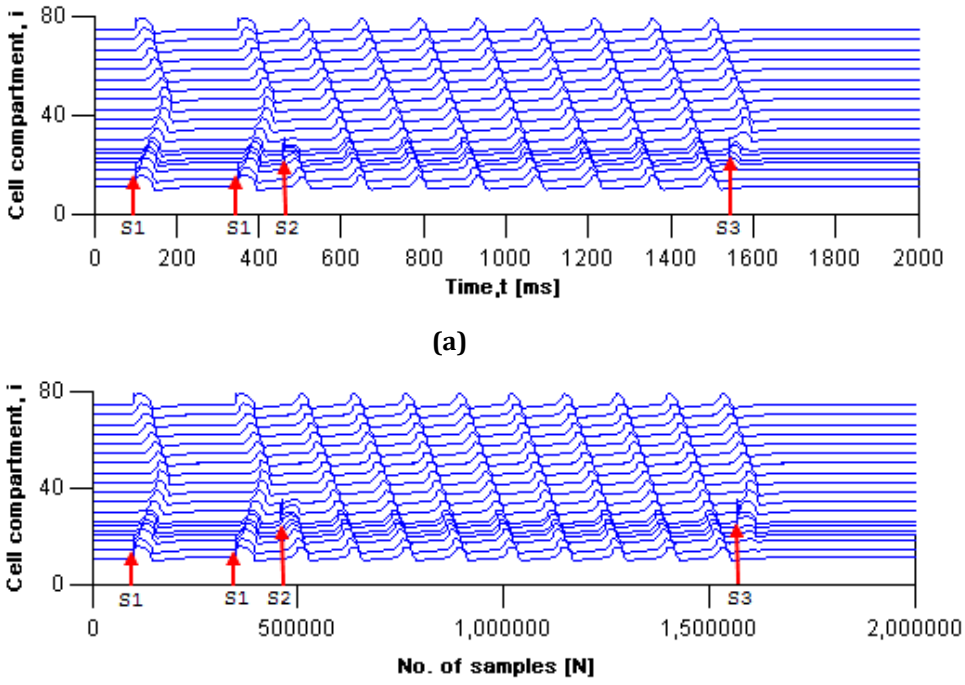

Fig. 2 *A space-time diagram showing membrane voltage as a function of time and position around the ring-shaped cable models. The membrane potentials have been recorded only for the compartments 1, 5, 10, 13, 15, 18, 20, 25, 30, 35, 40, 45, 50, 55, 60, 65, 70, 75 and 80. (a) MATLAB software-based computer simulation; (b) FPGA-on-board simulation*

3.2.2 Phase Resetting Curve (PRC) of Reentrant in the Ring-shaped Cable Model

Figure 3 shows the PRC of the (a) software-based computer simulation and (b) FPGA-on-board simulation. In both cases, the phase resetting has been largely negative (advance) when the stimulation phase was in the latter half of the reentry cycle. Moreover, only a small amount of the phase resetting could be found in the stimulation phase approximately between $0 < \varphi < 0.70$, with roughly $0 < t_{stim} < 90$ ms. Here, a stimulation phase close to 1 is corresponding to $t_{stim} \sim \bar{T}$ which indicates that the stimulation is delivered close to an oncoming wavefront of the reentry excitation. When a stimulation is applied around the middle of the cycle length, roughly $0.65 < \varphi < 0.80$ for the computer simulation and roughly $0.73 < \varphi < 0.77$ for FPGA-on-board simulation as depicted by vertical blue bands in Fig. 3(a) and (b), the reentry is annihilated by the stimulation as shown previously in Fig. 2(a) and (b). Here, the vertical blue band represents the annihilation phase in which the reentry is annihilated if a stimulation falls within this interval.

The similarity between both simulations is satisfied, although the PRC of the FPGA-on-board simulation is thought to be more precise compared to the software-based computer simulation since the model blocks in

Int. Journal of Integrated Engineering Vol. 16 No. 1 (2024) p. 272-281

MATLAB Simulink are defined as using a fixed-step solver with a fine step size of 0.001ms throughout the simulation.

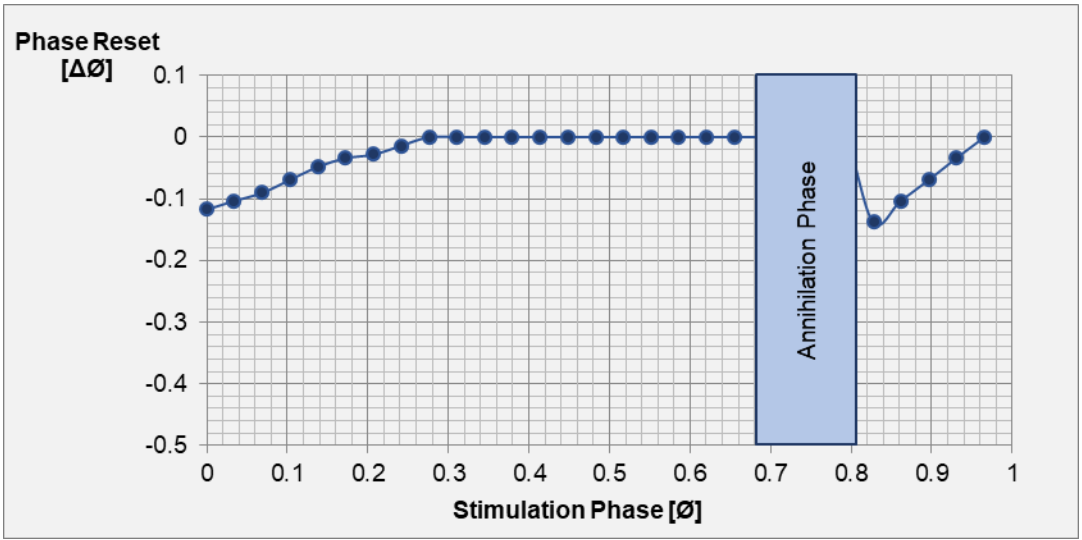

Fig. 3 *Representation of the PRCs that showing the amount of phase reset, Δφ against the stimulation phase, φ. (a) PRC of software-based computer simulation; (b) PRC of FPGA-on-board simulation, negative Δφ indicates phase advance*

4. Conclusion

According to the FPGA-on-board simulation on Xilinx Virtex-6, the action potential generation based on periodic trains of stimuli and the reentrant conduction based on the 1D ring-shaped cable model were favorably executed and analyzed, and they were comparable to those from the computer simulation. Furthermore, the simulation through the FPGA simulation can be done in real time compared to the time-consuming computer simulation. In the future, the implementation of other more complex cardiac models could provide a better solution in conducting the simulation-based cardiac electrical analysis using the FPGA. Moreover, a large scale and multidimensional cardiac conduction model in cardiac tissues or heart scale is required for better understanding in cardiac electrophysiology studies.

Acknowledgement

The authors would like to thank Universiti Tun Hussein Onn Malaysia through TIER 1 Grant No. Q359. Extended gratitude is expressed to Microelectronics & Nanotechnology - Shamsuddin Research Centre (MiNT-SRC) for the laboratory facilities.

Conflict of Interest

Authors declare that there is no conflict of interests regarding the publication of the paper.

Author Contribution

The authors confirm contribution to the paper as follows: ***study conception and design:*** *Farhanahani Mahmud, Nur Atiqah Adon, Norliza Othman, Mohamad Hairol Jabbar;* ***data collection:*** *Nur Atiqah Adon, Norliza Othman;* ***analysis and interpretation of results:*** *Farhanahani Mahmud, Nur Atiqah Adon, Norliza Othman, Mohamad Hairol Jabbar;* ***draft manuscript preparation:*** *Farhanahani Mahmud, Marlia Morsin. All authors reviewed the results and approved the final version of the manuscript.*

References

[1] Koshy, A. O., Gallivan, E. R., McGinlay, M., Straw, S., Drozd, M., Toms, A. G., ... & Witte, K. K. (2020). Prioritizing symptom management in the treatment of chronic heart failure. ESC Heart Failure, 7(5), 2193-2207.

[2] Leyva, F., Israel, C. W., & Singh, J. (2023). Declining Risk of Sudden Cardiac Death in Heart Failure: Fact or Myth?. Circulation, 147(9), 759-767.

[3] Koivumäki, J. T., Hoffman, J., Maleckar, M. M., Einevoll, G. T., & Sundnes, J. (2022). Computational cardiac physiology for new modelers: Origins, foundations, and future. Acta Physiologica, 236(2), e13865.
[4] Uzelac, I., Kaboudian, A., Iravanian, S., Siles-Paredes, J. G., Gumbart, J. C., Ashikaga, H., ... & Fenton, F. H. (2021). Quantifying arrhythmic long qt effects of hydroxychloroquine and azithromycin with whole-heart optical mapping and simulations. Heart Rhythm O2, 2(4), 394-404.
[5] Sorguven, E., Bozkurt, S., & Baldock, C. (2021). Computer simulations can replace in-vivo experiments for implantable medical devices. Physical and Engineering Sciences in Medicine, 44, 1-5.
[6] Hodgkin A.L. & Huxley A.F. (1952). A quantitative description of membrane current and its application to conduction and excitation in nerve. J. Physiol., 117, 500-544.
[7] Noble, D., Garny, A. & Noble P. J. (2012). How the Hodgkin-Huxley equations inspired the Cardiac Physiome Project. J.Physiol., 590(11), 2613-2628.
[8] Fitzhugh R. (1960). Thresholds and Plateaus in the Hodgkin-Huxley Nerve Equations. J. Gen. Physiol., 43, 867-896.
[9] Noble D. (1960). Cardiac action potential and pacemaker potentials based on the HodgkinHuxley equations. Nature, 188, 495-497.
[10] Beeler G.W. & Reuter H. (1977). Reconstruction of the action potential of ventricular myocardial fibres. J. Physiol., 268, 177-210.
[11] Luo, C. H. & Rudy, Y. (1991). A model of the ventricular cardiac action potential. Depolarization, repolarization, and their interaction. Circ. Research, 68(6), 1501-1526.
[12] Luo, C. H. & Rudy, Y. (1994). A dynamic model of the cardiac ventricular action potential. I. Simulations of ionic currents and concentration changes. Circ. Research, 74(6), 1071-1096.
[13] Luo, C. H., & Rudy, Y. (1998). A dynamic model of the cardiac ventricular action potential. II. Afterdepolarizations, triggered activity, and potentiation. Circulation research, 74(6), 1097-1113.
[14] Priebe, L. & Beuckelmann, D. J. (1998). Simulation Study of Cellular Electric Properties in Heart Failure. Circ. Research, 82(11), 1206–1223.
[15] Ten Tusscher, K. H., Noble, D., Noble, P. J. & Panfilov, A. V. (2004). A model for human ventricular tissue. American Journal of Physiology. Heart and Circulatory Physiology, 286(4), 1573-1589.
[16] Iyer, V., Mazhari, R. & Winslow, R. L. (2004). A computational model of the human left-ventricular epicardial myocyte. Biophys. Journal, 87(3), 1507-1525.
[17] Goel, A., Goel, A. K., & Kumar, A. (2023). Performance analysis of multiple input single layer neural network hardware chip. Multimedia Tools and Applications, 1-22.
[18] Chen, T., Schiek, M., Dammers, J., Shah, N. J., & van Waasen, S. (2020). Requirement-driven model-based development methodology applied to the design of a real-time MEG data processing unit. Software and Systems Modeling, 19, 1567-1587.
[19] Kumar, J. D., Babu, C. G., Balaji, V. R., & Visvesvaran, C. (2020, February). Analysis of effectiveness of power on refined numerical models of floating point arithmetic unit for biomedical applications. In IOP Conference Series: Materials Science and Engineering (Vol. 764, No. 1, p. 012032). IOP Publishing.
[20] Peccerillo, B., Mannino, M., Mondelli, A., & Bartolini, S. (2022). A survey on hardware accelerators: Taxonomy, trends, challenges, and perspectives. Journal of Systems Architecture, 129, 102561.
[21] Tavakkoli, V., Mohsenzadegan, K., Chedjou, J. C., & Kyamakya, K. (2020). Contribution to Speeding-Up the Solving of Nonlinear Ordinary Differential Equations on Parallel/Multi-Core Platforms for Sensing Systems. Sensors, 20(21), 6130.
[22] Xia,Y., Timothée, L. & Takashi, K. (2020). Digital Hardware Spiking Neuronal Network with STDP for Real-time Pattern Recognition. Journal of Robotics, Networking and Artificial Life, 7(2), 121-124.
[23] Abdoli, B. & Saeed,S. (2020). A reconfigurable real- time neuromorphic hardware for spiking winner- take-all network. International Journal of Circuit Theory and Applications, 48(12), 2141-2152.
[24] Gupta, S., Vyas, A. & Trivedi, G. (2020). FPGA Implementation of Simplified Spiking Neural Network, In 2020 27th IEEE International Conference on Electronics, Circuits and Systems (ICECS), 1-4.
[25] Lewis, B. J. (2023). Development of the Digital Signal Processing for the Space Weather Probes Version 2 Sensor Using the MATLAB/Simulink Environment.
[26] Norliza Othman, Farhanahani Mahmud, Abd Kadir Mahamad, Mohamad Hairol Jabbar & Nur Atiqah Adon. (2014). Cardiac Excitation Modeling: HDL Coder Optimization towards FPGA stand-alone Implementation. Proceedings of 2014 IEEE International Conference on Control System, Computing and Engineering, 436-440.
[27] N.A. Adon, F. Mahmud, M.H. Jabbar & N. Othman. (2014). FPGA-in-the-Loop Co-simulation of Reentrant Arrhythmia Mechanism in One Dimensional (1D) Ring-Shaped based on FitzHugh-Nagumo Model. Proceedings of 2014 IEEE International Conference on Control System, Computing and Engineering, 239-244.